Title
Mutant huntingtin impairs immune cell migration in Huntington disease

Journal
Journal of Clinical Investigation, 122(12)

ISSN
0021-9738

Authors
Kwan, Wanda
Träger, Ulrike
Davalos, Dimitrios
et al.

Publication Date
2012-12-03

DOI
10.1172/jci64484

Peer reviewed

Mutant huntingtin impairs immune cell migration in Huntington disease

Wanda Kwan,[1,2] Ulrike Träger,[3] Dimitrios Davalos,[2,4] Austin Chou,[2,5] Jill Bouchard,[2,5] Ralph Andre,[3] Aaron Miller,[6] Andreas Weiss,[7] Flaviano Giorgini,[6] Christine Cheah,[6] Thomas Möller,[8] Nephi Stella,[6,9] Katerina Akassoglou,[2,4,5,10] Sarah J. Tabrizi,[3] and Paul J. Muchowski[1,2,5,10,11,12]

[1]Biomedical Sciences Program, UCSF, San Francisco, California, USA. [2]Gladstone Institute of Neurological Disease, San Francisco, California, USA. [3]Department of Neurodegenerative Disease, UCL Institute of Neurology, London, United Kingdom. [4]Center for In Vivo Imaging Research, Gladstone Institute of Neurological Disease, San Francisco, California, USA. [5]Neuroscience Program, UCSF, San Francisco, California, USA. [6]Department of Pharmacology, University of Washington, Seattle, Washington, USA. [7]Neuroscience Discovery, Novartis Institutes for BioMedical Research, Basel, Switzerland. [8]Department of Neurology and [9]Department of Psychiatry and Behavioral Sciences, School of Medicine, University of Washington, Seattle, Washington, USA. [10]Department of Neurology and [11]Department of Biochemistry and Biophysics, UCSF, San Francisco, California, USA. [12]The Taube-Koret Center for Huntington's Disease Research, San Francisco, California, USA.

In Huntington disease (HD), immune cells are activated before symptoms arise; however, it is unclear how the expression of mutant huntingtin (htt) compromises the normal functions of immune cells. Here we report that primary microglia from early postnatal HD mice were profoundly impaired in their migration to chemotactic stimuli, and expression of a mutant htt fragment in microglial cell lines was sufficient to reproduce these deficits. Microglia expressing mutant htt had a retarded response to a laser-induced brain injury in vivo. Leukocyte recruitment was defective upon induction of peritonitis in HD mice at early disease stages and was normalized upon genetic deletion of mutant htt in immune cells. Migration was also strongly impaired in peripheral immune cells from pre-manifest human HD patients. Defective actin remodeling in immune cells expressing mutant htt likely contributed to their migration deficit. Our results suggest that these functional changes may contribute to immune dysfunction and neurodegeneration in HD, and may have implications for other polyglutamine expansion diseases in which mutant proteins are ubiquitously expressed.

Introduction

Huntington disease (HD) is a devastating, incurable neurodegenerative disease caused by a polyglutamine (polyQ) repeat expansion in htt, a ubiquitously expressed protein. HD is characterized by involuntary movements (chorea), personality and cognitive changes that are thought to arise from mutant huntingtin (htt)–induced neuronal dysfunction, and cell death in the striatum and cortex. However, mutant htt expression in non-neuronal cells in the brain and periphery may also contribute to HD pathogenesis (1–4). Indeed, a number of studies have documented specific pathology in an array of peripheral tissues from HD patients and mouse models. Abnormal phenotypes have been described in fibroblasts, red and white blood cells, and pancreatic, liver, muscle, and cardiac cells; tissues such as bones and testes are also affected (1, 2, 5). Abnormal energy metabolism, muscle wasting, and weight loss despite increased caloric intake are also invariable features of HD (6, 7).

Mutant htt is expressed at high levels in immune cells (8), and abnormalities in immune responses have been reported in patients with HD. Levels of soluble immune markers in serum, such as soluble TNF receptor, IL-2 receptor, and immunoglobulins, are elevated in HD patients (9, 10). Plasma samples from HD patients also have increased levels of proinflammatory cytokines and chemokines that correlate with disease progression (11, 12), occurring years before the onset of chorea and other HD symptoms. In response to an immune stimulus, monocytes and macrophages from HD patients and mouse models produce elevated levels of these proinflammatory factors (11). Transcription of genes in HD blood is also dysregulated and correlates with disease progression (1, 13–15). Finally, we recently showed that lethal irradiation coupled to bone marrow transplantation with WT cells normalizes levels of proinflammatory cytokines and chemokines and confers modest benefits in two mouse models of HD (16). These studies provide strong evidence that the peripheral immune system is abnormal in HD and might contribute to neurodegeneration.

Microglia, the resident immune cells in the brain, derive from the same hematopoietic stem cell lineage as peripheral myeloid cells; they are also abnormal in HD and may contribute to pathogenesis. Microglial activation and reactive gliosis occur in vulnerable regions of HD brains (17, 18). In the R6/2 HD mouse model, microglia were shown to be abnormal, as demonstrated by ferritin accumulation and Iba1 immunostaining, at early disease stages, and these abnormalities correlate with disease severity (19), which is indicative of cellular dysfunction (20); similar results were also observed in brains from mid-stage HD patients (19). Positron emission tomography of HD patients shows increased binding of ^{11}C-(R)-PK11195, a surrogate marker of microglial activation, in the striatum and cortex that correlates with loss of dopamine receptors and the clinical severity of the disease (21, 22). Furthermore, microglial activation in brain regions required for cognitive function can predict disease onset (23).

Immune cells undergo rapid morphological changes and migrate in response to pathological insults in tissues. The attraction of immune cells to chemotactic stimuli present at sites of infection or injury is an early and essential step in immune responses. Activated immune cells localize in affected tissues and communicate through short-range cytokines and cell-cell contact (24). Immune cells such as monocytes, macrophages, and microglia express chemoattractant receptors and adhesion molecules that control and direct migration in response to inflammatory cues (25). These cells rely on the remod-

Conflict of interest: The authors have declared that no conflict of interest exists.
Citation for this article: *J Clin Invest.* 2012;122(12):4737–4747. doi:10.1172/JCI64484.

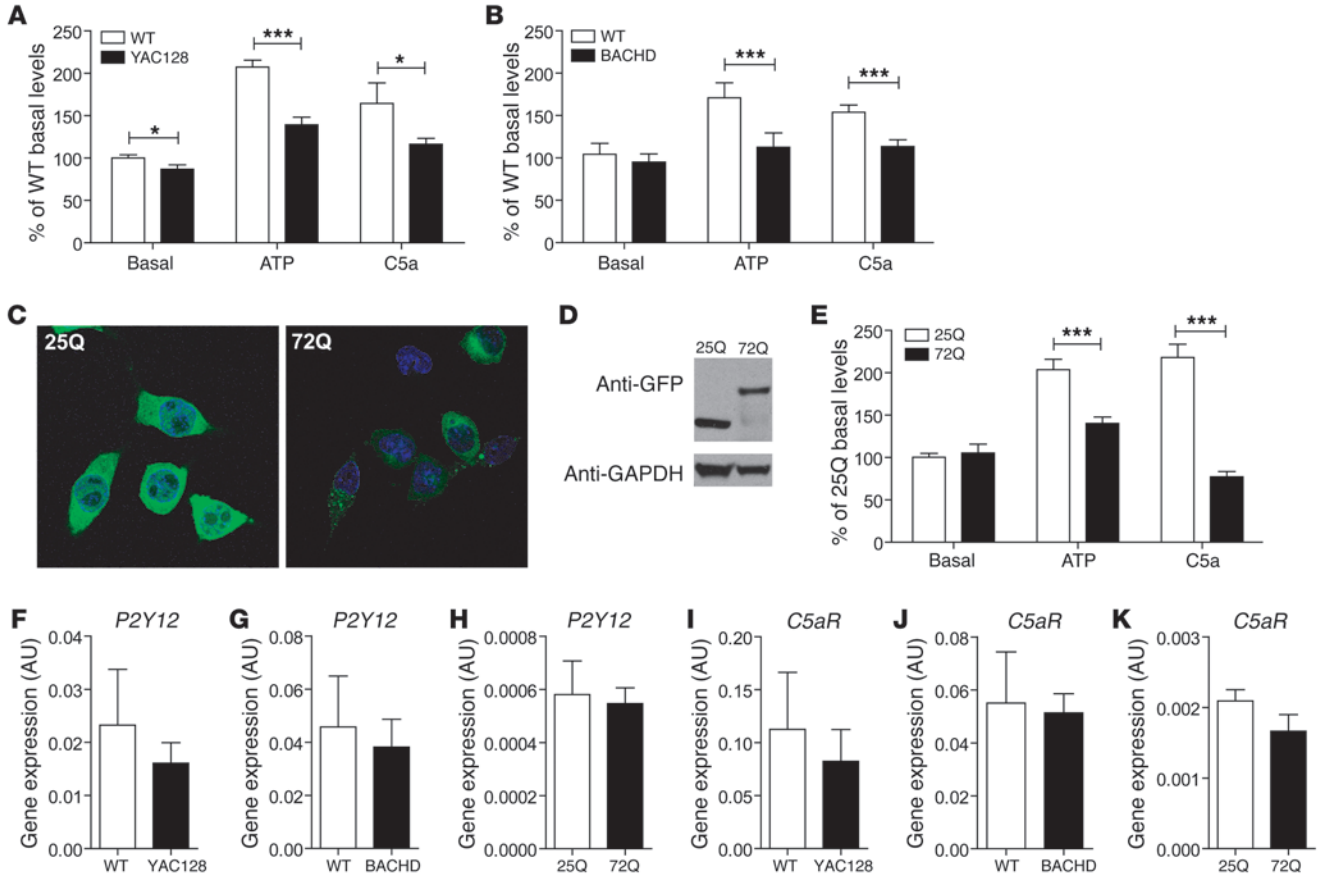

Figure 1

Mutant htt expression in microglia impairs their chemotactic response to ATP and C5a. Primary microglia from (**A**) YAC128 and (**B**) BACHD mice show significant migration defects in response to ATP (100 μM) and C5a (100 nM) compared with WT cells. (**C**) BV2 microglial cell lines were stably transduced with lentiviral constructs that express GFP-tagged mutant htt fragments of 25Q and 72Q (total original magnification, ×600). (**D**) Transgene expression was confirmed by Western blot analysis with anti-GFP. (**E**) A BV2 microglial cell line expressing htt 72Q shows a similar migration defect in response to these stimuli compared with htt 25Q–expressing cells. Cells were cultured in a Boyden chamber and allowed to migrate through the filter for 3 hours. Values are mean ± SEM. $n > 6$ experimental replicates; $^*P < 0.05$, $^{***}P < 0.001$ (*t* test). (**F**–**K**) Gene expression levels of *P2Y12* and *C5aR*, the cognate receptors for ATP and C5a, respectively, were not significantly different in YAC128 (**F** and **I**), BACHD (**G** and **J**) microglia, and microglia expressing htt 72Q (**H** and **K**) when compared with the WT controls. Values are mean ± SEM. $n = 3$–4 experimental replicates.

eling of the actin cytoskeleton, a key mediator of cell polarization and chemotaxis (26, 27). Transmigration of peripheral immune cells from the bloodstream into perivascular tissue allows their accumulation at the site of injury or infection (24). In the brain, microglia quickly rearrange their actin networks and form membrane ruffles and leading edges for process extension and chemotaxis (28, 29). In vivo imaging studies on microglia using 2-photon microscopy showed that these cells respond rapidly by extending their processes toward a laser ablation injury (30). Even in healthy brain, microglia continuously extend and retract their processes to actively survey their microenvironment (31). They also provide trophic support for neurons and physically interact with synapses (32). Overall, the migration of immune cells is a critical step during the initial response to injury or inflammation, and defects in cell migration prevent appropriate responses to infections (33, 34).

In this study, we tested the hypothesis that mutant htt impairs the function of microglia and peripheral myeloid cells. Our data indicate that immune cells expressing mutant htt have impaired migration in vitro and in vivo, and that migration defects may be due in part to perturbations in actin remodeling. Thus, expression of mutant htt in microglia and immune cells may cause cell-autonomous deficits that could participate in the pathogenesis of HD.

Results

Mutant htt expression in microglia impairs migration to chemotactic stimuli. YAC128 and BACHD mice are well-characterized mouse models of HD that express full-length htt and recapitulate many behavioral and pathological features of the disease (35, 36). To analyze the migration of microglia that express mutant htt, we isolated primary microglia from the brains of YAC128 and BACHD mice and tested these cells in a Boyden chamber assay. In this assay, cells that transmigrate from one chamber toward a chemoattractant in a second chamber are trapped in a filter. Microglia were stained with the fluorescent dye DRAQ5, and the number of cells that had migrated was determined by measuring the fluorescence intensity. In the absence of a chemoattractant, YAC128 microglia showed modestly less

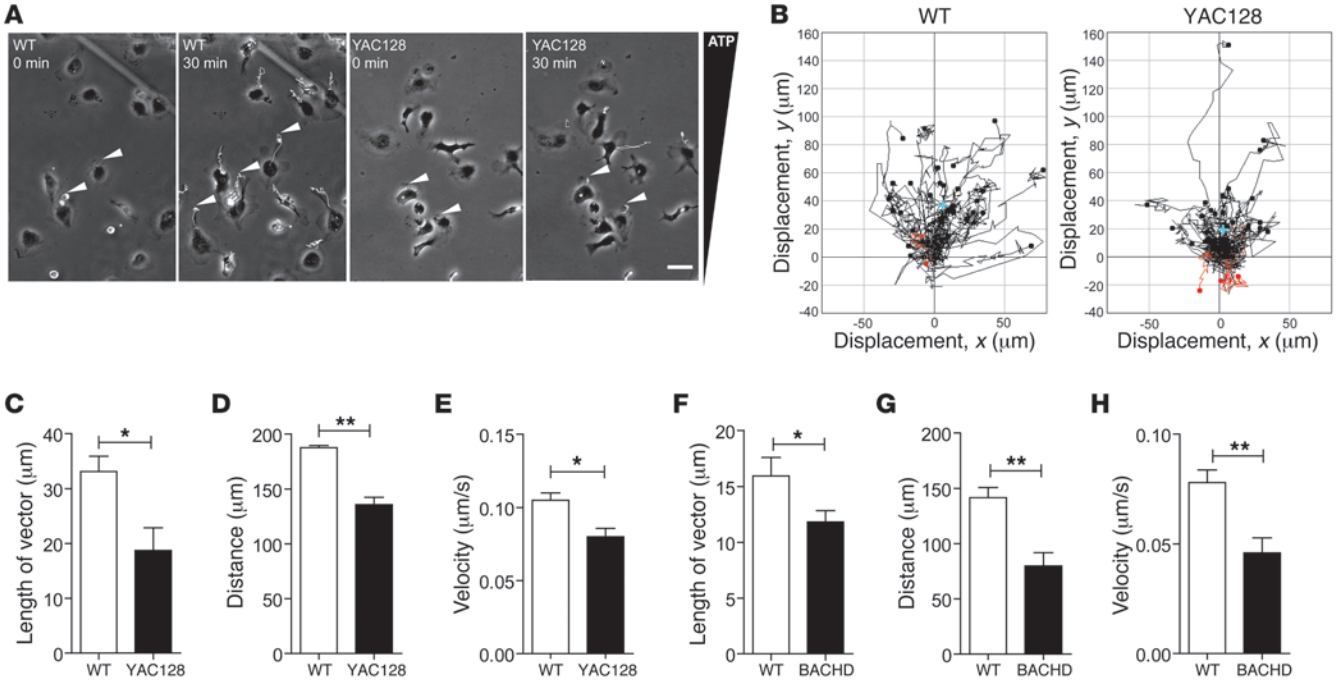

Figure 2

Mutant htt expression in microglia diminishes the extension of microglial processes toward ATP. (**A**) Microglia from WT and YAC128 mice were placed in a gradient of ATP (0–100 μM) in a Dunn chemotaxis chamber and imaged by phase contrast, time-lapse microscopy. Microglia from WT mice show robust extension of processes (arrowheads) toward the ATP gradient (white lines indicate the movement of the leading edge of cell over 30 minutes); the response of YAC128 microglia is significantly decreased. (**B**) Chemotaxis plots showing tracks and distance (μm) traveled by the leading edge of WT (left) and YAC128 (right) microglia toward ATP after 30 minutes. Values are plotted in the *x* and *y* directions relative to the starting location. Black lines indicate a net extension; red lines indicate a net retraction; light blue cross indicates the mean length of the vector. (**C**–**H**) Summary of the mean length of the vector (**C** and **F**), mean velocity (**D** and **G**), and mean accumulated distance (**E** and **H**) of WT and YAC128 microglia ($n = 2$; 3 independent experiments), and WT and BACHD microglia ($n = 6$; 5 independent experiments). For each sample in each experiment the processes of at least 30 microglial cells were analyzed. Values are mean ± SEM. $^*P < 0.05$, $^{**}P < 0.01$ (*t* test). Scale bar: 50 μm.

basal migration than cells from WT littermate controls; BACHD microglia showed no deficit in basal migration (Figure 1, A and B). In contrast, upon exposure to the chemoattractants ATP (100 μM) and complement protein C5a (100 nM), microglia from YAC128 and BACHD mice displayed a highly significant decrease in migration relative to cells from WT littermates (Figure 1, A and B).

To determine whether expression of a mutant htt fragment in microglia could elicit migration deficits, we generated stable microglial cell lines (BV2 cells) that express GFP-tagged htt exon 1 with 25Q or 72Q (ref. 37 and Figure 1, C and D). Similar to neurons, microglial cell lines expressing htt 72Q contained inclusion bodies (Figure 1C), but they did not differ in proliferation compared with htt 25Q controls (data not shown). We tested the migration response of these cells in the Boyden chamber assay. As in YAC128 and BACHD mice, cells expressing a 72Q mutant htt fragment showed a severe reduction in migration in response to ATP or C5a relative to cells expressing a 25Q htt fragment (Figure 1E).

Quantitative PCR revealed that microglia expressing mutant htt showed a trend toward decreased mRNA levels of *P2Y12*, the purinergic receptor that mediates their migration response to ATP (38, 39), and the C5a receptor (Figure 1, F–K). Since C5a and ATP stimulate microglial migration through different downstream signaling pathways (40), these results suggest that migration deficits in microglia expressing mutant htt are not likely due to a lack of chemoattractant receptor expression, but rather may reflect an impaired ability to engage downstream signaling mechanisms and machinery required for proper migration. Notably, since similar results were found in microglia that express full-length mutant htt and those expressing mutant htt fragment, these results may suggest that similar mechanisms of migration impairment may occur in both mutant htt models.

Mutant htt impairs process extension in microglia. Next, we used time-lapse microscopy to assess the ability of microglia to extend processes and migrate in response to an ATP gradient (0–100 μM) in a Dunn chemotaxis chamber. The Dunn chemotaxis chamber allows the behavior of cells subjected to a linear concentration gradient of chemoattractant to be observed directly by microscopy. In this assay, microglia from WT mice had clear and robust polarization of their leading edges toward the ATP source within 30 minutes, whereas YAC128 microglia had a substantial reduction in the extension and movement of their processes (Figure 2, A and B, and Supplemental Videos 1 and 2; supplemental material available online with this article; doi:10.1172/JCI64484DS1). By tracking the path and leading edge displacement of each cell, we determined the average distance and *x*- and *y*-axis displacements of cells. The mean length of overall process displacement in YAC128 microglia was significantly reduced, as were the mean velocity of cellular movement and the mean overall accumulated distance of the processes (Figure 2, C–E). Similar results were obtained in BACHD microglia (Figure 2, F–H). Thus, migration deficits in mutant htt–express-

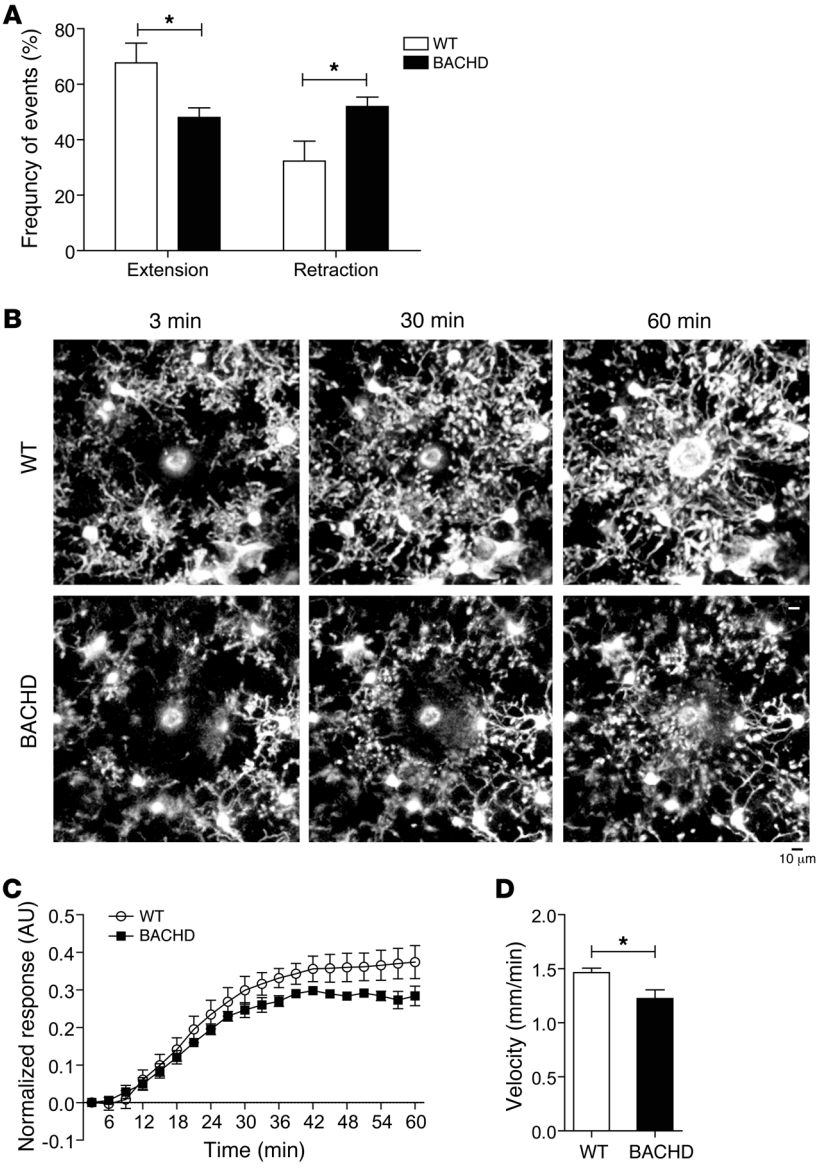

Figure 3
Microglia show defective basal process dynamics and delayed responses to focal laser ablation in the cortex of BACHD mice in vivo. Microglia from WT;*Cx3cr1*$^{GFP/+}$ (WT) or BACHD$^{Tg/+}$;*Cx3cr1*$^{GFP/+}$ (BACHD) mice were imaged in vivo using 2-photon microscopy at 12–18 months of age. (**A**) Baseline time-lapse imaging of microglia demonstrated reduced extension and increased retraction of microglial processes over 10 minutes in BACHD$^{Tg/+}$;*Cx3cr1*$^{GFP/+}$ compared with WT;*Cx3cr1*$^{GFP/+}$ control mice. *$P < 0.05$ (*t* test). (**B**) Tissue ablation with a laser (white zone in center) results in rapid extension of microglial processes toward the site of injury in WT;*Cx3cr1*$^{GFP/+}$ mice. In contrast, microglia from BACHD$^{Tg/+}$;*Cx3cr1*$^{GFP/+}$ mice show a delayed response over a 60-minute period. (**C**) Quantification of process extension toward the site of laser ablation. $P < 0.001$ (2-way ANOVA). (**D**) The average velocity of process extension is significantly decreased in microglia from BACHD$^{Tg/+}$*Cx3cr1*$^{GFP/+}$ mice over a 45-minute period. *$P < 0.05$ (*t* test). Values are mean ± SEM. $n = 4–5$ mice. Scale bar: 10 μm.

ing microglia are likely due to defective process polarization and extension. Interestingly, although the vast majority of mutant htt–expressing microglia did not extend and move their processes as efficiently as cells from WT littermate controls, a very small number of cells had extensive process displacement, suggesting that migration defects elicited by mutant htt may not be fully penetrant, perhaps due to cell-to-cell variability in mutant htt levels.

Mutant htt impairs microglial function in vivo. To validate our in vitro results, we measured microglial process extension and retraction in the intact cortex of 12- to 18-month-old BACHD mice by time-lapse in vivo imaging using 2-photon microscopy. *Cx3cr1* encodes for the fractalkine receptor, which is highly expressed in microglia and moderately expressed in monocytes. *Cx3cr1*$^{GFP/+}$ mice have been used previously to image brain microglia in living mice (30). Here, we fluorescently labeled microglia by generating BACHD$^{Tg/+}$;*Cx3cr1*$^{GFP/+}$ mice.

Under basal conditions, process extension was less frequent, and process retraction was more frequent in BACHD$^{Tg/+}$;*Cx3cr1*$^{GFP/+}$ mice than in controls (WT;*Cx3cr1*$^{GFP/+}$) ($P < 0.01$) (Figure 3A). Microglial cell size and density were not significantly different in the two groups (data not shown). In response to brain injury induced by focal laser ablation, microglia from WT control mice showed a robust response characterized by the rapid extension of processes and eventual engulfment of the injury site as described previously (30, 38). In contrast, microglia from BACHD$^{Tg/+}$;*Cx3cr1*$^{GFP/+}$ mice were unable to fully encompass the site of injury, and the response was significantly delayed ($P < 0.001$) (Figure 3, B and C, and Supplemental Videos 3 and 4). Indeed, the mean velocity of microglial processes in BACHD$^{Tg/+}$;*Cx3cr1*$^{GFP/+}$ mice over the first 45 minutes (the average duration of the microglial process extension to reach the ablation site in WT mice) was approximately 20% lower than that in control mice (Figure 3D). Thus, microglia present significant functional impairment in the brains of aged BACHD mice, both in their tissue surveillance behavior under unperturbed conditions and in their ability to rapidly respond to and contain a localized brain injury.

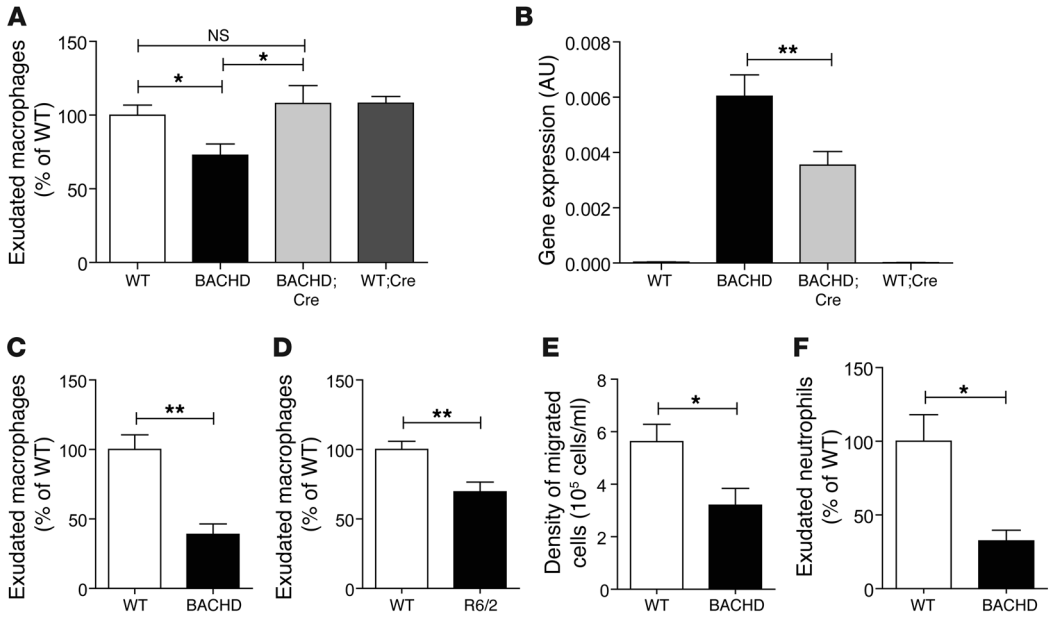

Figure 4

The migration of macrophages to the peritoneum in response to thioglycollate is defective in mouse models of HD. Thioglycollate (3%) was injected into the peritoneum of HD mice, and cells were harvested after 24 or 48 hours. (**A**) At 6–9 weeks, BACHD mice have a marked reduction in peritoneal macrophage recruitment. This defect was completely normalized in BACHD$^{Tg/+}$;*CD11b-Cre* (BACHD;Cre) mice, in which mutant htt expression is absent in CD11b-expressing cells. Values are mean ± SEM. n = 20, 14, 7, and 15 for WT, BACHD, BACHD$^{Tg/+}$;*CD11b-Cre*, and WT;*CD11b-Cre* (WT;Cre), respectively. *P < 0.05 (1-way ANOVA, Bonferroni's post hoc test). (**B**) Mutant *Htt* gene expression is decreased in peritoneal exudates from BACHD$^{Tg/+}$;*CD11b-Cre* mice compared with BACHD. Values are mean ± SEM. n > 3. **P < 0.01 (1-way ANOVA, Bonferroni's post hoc test). (**C** and **D**) Macrophage recruitment was also decreased in (**C**) BACHD at 8–10 months (WT, n = 3; BACHD, n = 5) and (**D**) R6/2 mice at 8 weeks (WT, n = 16; R6/2, n = 15). For evaluation of macrophage recruitment, cells were stained with anti-F4/80–APC and analyzed by FACS. Recruited populations were expressed as the percentage of F4/80^{dim} cells to total cells. (**E** and **F**) The density of total infiltrating cells (**E**) and exudate neutrophils (Gr-1$^+$ cells within the CD11b population) (**F**) is also lower in BACHD mice than in controls. Results are normalized to WT controls. Values are mean ± SEM, n = 6–18. *P < 0.05, **P < 0.01 (t test). n represents number of mice used.

Migration of macrophages to an inflammatory stimulus is impaired in mouse models of HD. Microglia, macrophages, and monocytes are mononuclear phagocytes thought to be derived from the same myeloid progenitor cell (41–43). To determine whether the migration of peripheral macrophages is also impaired in HD mouse models, we evaluated the in vivo recruitment of macrophages in response to a peritoneal injection of thioglycollate (a nonspecific inflammatory stimulus). Cells were collected from the peritoneum and labeled for the macrophage marker F4/80, and the F4/80^{dim} population (infiltrating macrophages) was quantified by fluorescence-activated cell sorting (FACS). At 6–9 weeks of age, macrophage recruitment in response to thioglycollate in BACHD mice was markedly (~27%) reduced (Figure 4A). To determine whether mutant htt expression was necessary for deficits in migration, we used a genetic approach whereby mutant htt expression in macrophages is deleted by breeding BACHD mice, which have Cre recombinase excision (*loxP*) sites flanking the coding sequence for mutant htt (36), with *CD11b-Cre* transgenic mice, which express Cre recombinase in myeloid lineage cells including macrophages (44). Importantly, the recruitment of macrophages to the peritoneum was normalized in BACHD$^{Tg/+}$;*CD11b-Cre* mice (Figure 4A). We further confirmed that mutant htt expression is partially but significantly decreased in peritoneal exudates from BACHD$^{Tg/+}$;*CD11b-Cre* mice compared with BACHD$^{Tg/+}$ mice (Figure 4B). The residual mutant htt expression in peritoneal exudates in BACHD$^{Tg/+}$;*CD11b-Cre* mice could be contributed by the CD11b$^-$ population. Although our data do not definitively rule out the contribution of a potential migration defect in other mutant htt–expressing cells in the peritoneal exudate (i.e., CD11b$^-$ cells), the results are consistent with the hypothesis that migration deficits of macrophages in BACHD mice are contributed by their expression of mutant htt. Significantly decreased macrophage recruitment to the peritoneum was also observed in older BACHD mice (8–10 months of age) (Figure 4C) and in the R6/2 transgenic mouse model of HD, which expresses mutant htt exon 1 (Figure 4D). Together, these results suggest that peritoneal macrophage infiltration in response to an inflammatory stimulus is strongly impaired in two mouse models of HD and likely caused by a cell-autonomous effect of mutant htt in these cells.

As thioglycollate-induced peritonitis can also lead to recruitment of neutrophils and other leukocytes, we determined whether migration of other cell types was also impaired in BACHD mice. We found fewer total infiltrating cells in the peritoneum of BACHD than in WT mice and approximately 60% fewer neutrophils, as shown by labeling with the neutrophil marker Gr-1 (Figure 4, E and F). These findings indicate that migration deficits are not restricted to macrophages in HD mouse models, but are also found in other cells of the myeloid lineage.

Monocytes and macrophages from HD patients display migration defects. To determine whether impaired migration of immune cells occurs in HD patients, we isolated monocytes from the blood of HD

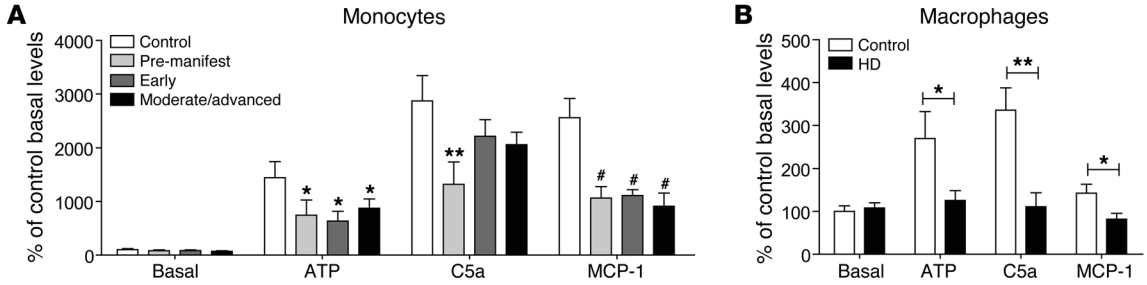

Figure 5

Severe impairment in migration of monocytes and macrophages isolated from HD patients. (**A**) Monocytes and (**B**) macrophages were isolated or derived from blood samples of presymptomatic HD patients, HD patients with early and moderate/advanced symptoms, and age-matched controls and assayed for migration using a Transwell approach. Cells from HD patients have significantly impaired migration relative to the control upon stimulation with ATP (100 μM), C5a (10 nM), and MCP-1 (50 ng/ml). Results are normalized to control basal levels. Values are mean ± SEM. $n > 4$ patient samples. $^{*}P < 0.05$, $^{**}P < 0.01$ (2-way ANOVA, Bonferroni post hoc test), $^{\#}P < 0.001$.

patients at various disease stages (Supplemental Tables 1 and 2) and used a Transwell approach to test the migration of these cells toward chemoattractants. Like microglia from HD mice, monocytes from presymptomatic HD patients were markedly impaired in their migration toward ATP (Figure 5A). Monocytes from HD patients were also impaired in their migration to monocyte chemoattractant protein–1 (MCP-1), a chemokine that recruits monocytes to sites of inflammation (Figure 5A). The magnitude of the migration deficit was similar in monocytes from early and moderate/advanced HD patients upon stimulation with ATP and MCP-1. Although there was significant migration impairment in cells isolated from presymptomatic HD patients toward the complement protein C5a, advanced-stage patients showed only a trend toward a significant decrease (Figure 5A). Macrophages differentiated from monocytes of HD patients by stimulation with GM-CSF also showed impaired migration toward ATP, C5a, and MCP-1 (Figure 5B). These results indicate that the migration of monocytes and macrophages isolated from HD patient blood to chemotactic stimuli is severely impaired.

Impaired actin remodeling in microglia from HD mouse models. When microglia and other myeloid cells migrate toward chemotactic stimuli, they rapidly reorganize the actin cytoskeleton and plasma membrane in a process referred to as membrane ruffling, typically before a lamellipodium forms. We hypothesized that the migration deficits in microglia and peripheral immune cells that express mutant htt were caused by perturbations in cytoskeletal dynamics induced by mutant htt. To test this hypothesis, we isolated primary microglia from HD mouse models, stained actin in the cells with rhodamine-phalloidin, and quantified the fraction of cells with membrane ruffling. Upon stimulation with ATP (100 μM) for 10 minutes, membrane ruffling in YAC128 microglia was significantly reduced ($P < 0.01$) (Figure 6A). We also determined whether YAC128 microglia were sensitive to stimulation with M-CSF (100 ng/ml), which induces membrane ruffling through Rac-mediated activation of actin polymerization as opposed to the G-protein–coupled receptor pathways that are transduced by ATP (39, 45, 46). Treatment with M-CSF increased membrane ruffling more than 3-fold in WT microglia but had no effect on microglia from YAC128 mice (Figure 6A). This response induced by ATP and M-CSF was also impaired in BACHD microglia (Figure 6, B and C).

The actin-binding protein cofilin is essential for the regulation of actin depolymerization and is required for effective cell migration (47). Cofilin undergoes active phosphorylation and dephosphorylation in response to stimuli, such as ATP, that trigger changes in the actin cytoskeleton. Cofilin phosphatase activity is measured by a decrease in phosphorylated cofilin (p-cofilin) immunoreactivity upon ATP stimulation (48). Under basal conditions, p-cofilin expression in primary microglia from BACHD mice was already significantly lower than that of WT littermates (Figure 6, D and E). Upon ATP stimulation, primary microglia from BACHD mice also lacked the transient/dynamic change that occurred in WT cells after 10 and 20 minutes (Figure 6, D and G), suggesting defective actin remodeling. Total cofilin levels were also decreased in primary microglia from BACHD mice (Figure 6, D and F), in N9 microglial cell lines that stably express mutant htt 72Q (Figure 6H), and in brain homogenates from BACHD mice (Figure 6I). We further confirmed that cofilin levels were decreased in peritoneal macrophages isolated from BACHD mice (Figure 6J). Our results suggest that expression of mutant htt in microglia impairs actin remodeling by decreasing levels of cofilin and p-cofilin in a manner that might contribute to migration deficits, consistent with a recent study reporting that mutant htt impairs actin remodeling during stress (49). In contrast to the protein levels, cofilin mRNA levels were not significantly different in primary microglia from BACHD mice (Figure 6K) and peritoneal macrophages (Figure 6L). Overall, our results suggest that mutant htt in microglia may influence cofilin levels primarily by a post-transcriptional mechanism, thereby affecting the actin signaling mechanisms associated with cofilin.

Discussion

Activation of the innate immune system has been reported in HD patients, yet it is unclear whether this is due to the effect of mutant htt or represents a secondary event in response to the degeneration of neurons. As evidenced by isolated primary HD microglia culture assays, microglial cells lines with overexpression of mutant htt, isolated human HD myeloid cells, and in vivo thioglycollate assays in HD mice, our results demonstrate that myeloid cells expressing mutant htt exhibit deficits in migration to chemotactic stimuli. Our results also suggest that these deficits are dependent on mutant htt expression. Migration deficits were observed in primary microglia when isolated from *early* postnatal HD mice, prior to any significant cell loss, consistent with apparent microglial dysfunction observed in pre-manifest HD patients (19, 21–23, 50). Importantly, migration deficits were observed in monocytes and macrophages isolated from HD patients before the onset of

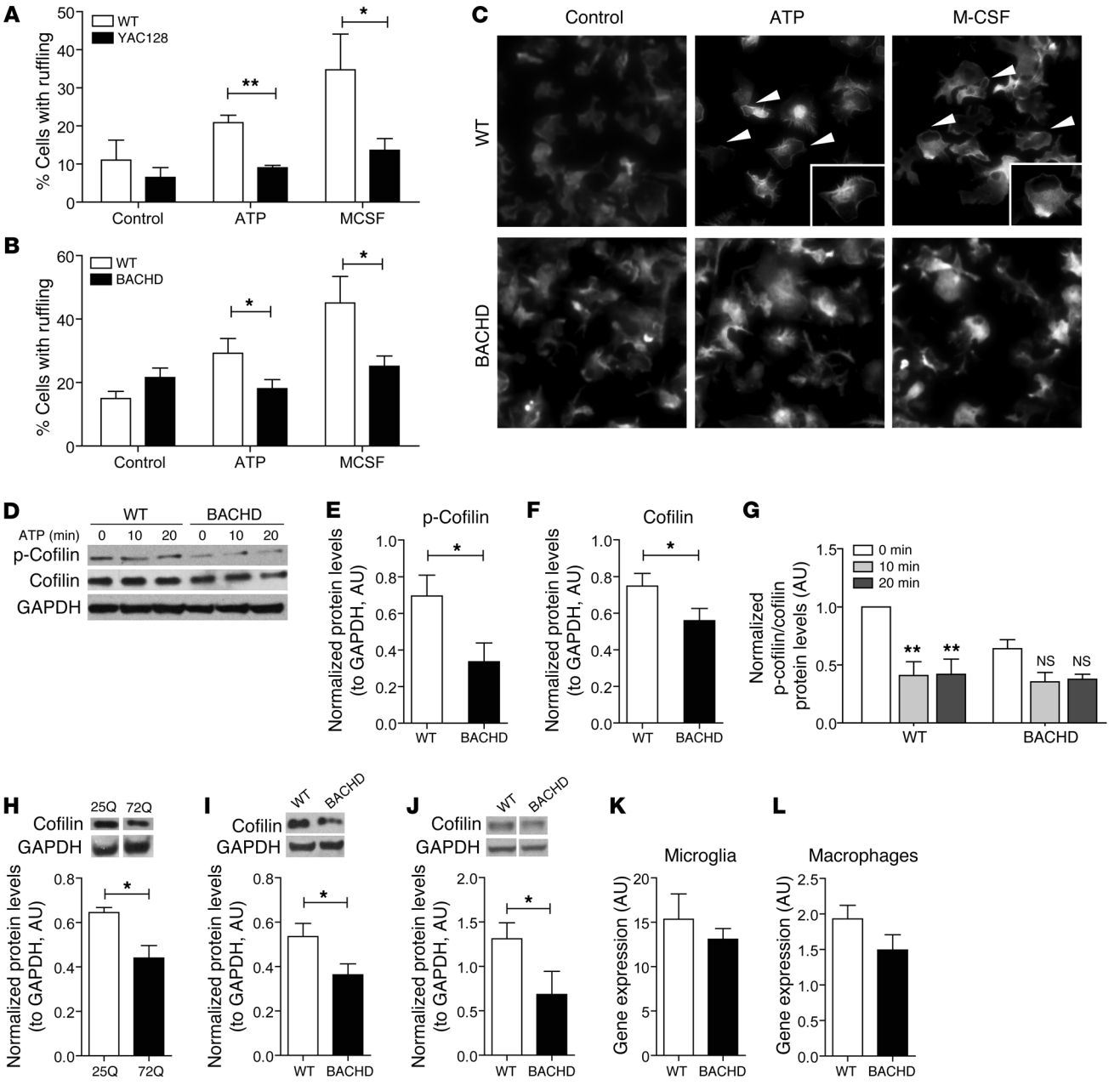

Figure 6

Mutant htt expression in microglia decreases membrane ruffling and cofilin levels. Primary microglia from (**A**) YAC128 and (**B**) BACHD mice have less membrane ruffling upon stimulation with ATP (100 μM) and M-CSF (100 ng/ml) than WT microglia. Membrane ruffling did not differ in HD microglia treated with M-CSF and untreated cells. Cells were stained with rhodamine-phalloidin, and the percentage of cells with membrane ruffling was quantified within 10 minutes. Values are mean ± SEM of 3 independent experiments. $^*P < 0.05$, $^{**}P < 0.01$ (*t* test). (**C**) Representative images of WT and BACHD microglia stained with rhodamine-phalloidin (total original magnification, ×200). Membrane rufflings (white arrows) are indicated as distinct white lines at the perimeter of the cells, while cells without membrane ruffling have dispersed phalloidin staining. Inset is a ×1.5 zoom of the cell of interest in the corresponding image. (**D**) Western blot analysis, performed with antibodies against p-cofilin, cofilin, and GAPDH, of homogenates from primary microglia isolated from BACHD mice at selected times after stimulation with ATP (100 μM). (**E** and **F**) p-Cofilin and cofilin baseline levels are lower in primary BACHD than WT microglia. (**G**) BACHD microglia do not have the robust dynamic change in p-cofilin upon ATP stimulation. Data were quantified as the ratio of p-cofilin to cofilin, both normalized to GAPDH levels. (**H**–**J**) Western blot analysis with an antibody against cofilin shows lower cofilin protein levels in (**H**) N9 microglial cell lines expressing htt 72Q, (**I**) BACHD brain homogenates, and (**J**) BACHD peritoneal macrophages than in controls ($^*P < 0.05$). Protein levels were normalized to GAPDH levels. (**K** and **L**) Cofilin mRNA levels are not significantly decreased in primary BACHD microglia and BACHD peritoneal macrophages. Values are mean ± SEM. *n* = 3–5 biological replicates (*t* test).

neurological and motor symptoms, and these deficits appeared to be independent of disease stage. Similar results were observed in vivo in mouse models of HD.

The detailed molecular mechanisms responsible for migration defects in immune cells that express mutant htt are likely to be complex and remain to be fully elucidated. However, our data suggest that mutant htt perturbs the proper regulation of actin remodeling due to decreased levels of cofilin and p-cofilin. Consistent with our findings in microglia, mutant htt colocalizes with nuclear actin-cofilin rods in neurons under conditions of stress (49). This study also detected cross-linked complexes of actin and cofilin in HD patient lymphoblasts that correlated with disease progression. Although mutant htt may directly interact with cofilin and actin in microglia and peripheral myeloid cells, cofilin was reported to physically interact only with full-length mutant htt and not mutant htt fragments (49). On the other hand, we showed reduced cofilin levels in both mutant full-length htt– and fragment htt–expressing microglia. Because we found that the phosphatase activity also appears to be altered upon ATP stimulation, it is conceivable that mutant htt may also affect the kinase that phosphorylates cofilin and/or other components of the actin remodeling machinery. As reported, in non-stimulated conditions, membrane ruffling and actin polymerization are reduced in the dendritic spines and synapses of striatal neurons from HD mouse models (51, 52). Since membrane ruffling is not altered in HD microglia in the absence of stimulation, the functional effect of mutant htt on actin remodeling may be different from that in neurons. Cytoskeletal organization is needed for normal neuronal cell development and functionality, and perhaps neurons are more sensitive to mutant htt effects under basal conditions. Moreover, the effects of mutant htt and the normal functions of htt on actin remodeling may vary between neurons and immune cells. Interestingly, null mutants of htt in *Dictyostelium discoideum* are also impaired in polarization and chemotaxis, suggesting that migration impairment in mutant htt–expressing immune cells could be due at least in part to the loss of WT htt function (53).

Our observations of migration deficits in microglia and peripheral myeloid cells that express mutant htt may have important implications for understanding HD pathogenesis. Under basal conditions in the intact healthy brain, microglia represent "sentinels" whose highly motile processes constantly survey the brain parenchyma and make transient activity-dependent contacts with synapses (31, 32). One recent study suggests that microglial activation with ATP triggers astrocyte-mediated modulation of excitatory neurotransmission (54). Microglia have dysfunctional morphological phenotypes and are aberrantly activated early in HD patients and mice. Interestingly, microglia from mice that lack both copies of the chemokine receptor *Cx3cr1* (*Cx3cr1*$^{GFP/GFP}$), which functions in leukocyte trafficking, also have activated morphological phenotypes (55). We show that microglia harvested from early *postnatal* HD mice already have defects in process extension and migration, suggesting this impairment could contribute to the early activation phenotypes reported in the HD brain. In addition, under basal, unperturbed conditions, microglia from adult BACHD mice exhibited significant deficits in process extension and exaggerated process retraction. Since synapse levels are decreased in BACHD mice (16) and other HD mouse models (56), these results suggest that microglia expressing mutant htt may not be efficient in synapse surveillance, which could conceivably contribute to synaptic and network dysfunction. We also found that microglia from aged BACHD mice showed a delayed response to laser-induced injury. As microglia form the first line of defense in the CNS by orchestrating rapid responses aimed to contain pathological insults within the normal brain (30, 31), these results suggest that mutant htt–expressing microglia might be limited in their ability to respond to traumatic or pathological insults, such as traumatic brain injury or brain infections. Taken together, our results indicate that migration impairment in microglia may be one of the first abnormalities in the HD brain, thereby compromising the functional integrity of the HD brain in early and late stages.

Mutant htt expression in peripheral myeloid cells might also contribute to some aspects of central and peripheral pathogenesis in HD. Proinflammatory cytokines and chemokines are elevated in pre-manifest HD patients and remain elevated throughout the course of disease (11, 12). We hypothesize that migration deficits in immune cells may lead to inefficient transduction of cytokine and chemokine signaling mechanisms, which may explain chronic increases in proinflammatory cytokines and chemokines and microglial activation in HD patients. Indeed, IL-6, IL-8, IL-1β, TNF-α, and MCP-1 levels are elevated in HD and are predicted to augment inflammatory signals in the brain. These factors could also contribute directly to neuronal dysfunction, as receptors for many of these molecules are expressed on neurons, some of which transduce proapoptotic signaling pathways (57, 58). Consistent with this hypothesis, myeloid cells in mice mutant for the chemokine receptor *Cx3cr1* are impaired in migration, leading to increased IL-1β levels and decreased synaptic plasticity (55, 59). In mice with deletion of Ccr2, whose monocytes and macrophages also do not migrate properly, serum levels of IL-6 and IL-1β are elevated (33, 60). Mice mutant for these chemokine receptors are also unable to clear infections, have impaired wound healing, and are unable to mount effective adaptive immune responses (33, 61–63). Unfortunately, no studies to date have systematically examined whether the incidence of infections or defects in wound healing are increased in HD patients, although chronic skin ulcers have been reported (64). Ongoing studies in our laboratory are examining whether HD mice can efficiently clear bacterial and viral infections, and if infections influence degenerative processes in the CNS and periphery.

Several recent studies in mouse models provide additional support for the hypothesis that dysfunction of the peripheral immune system might play an important disease-modifying role in HD. Proinflammatory cytokines did not increase in YAC128 mice that received transplants of WT bone marrow, and this conferred modest behavioral and neuropathological benefits to YAC128 and BACHD mice (16). Genetic deletion of cannabinoid receptor 2 (CB2) — a protein expressed predominantly in peripheral immune cells that regulates production of proinflammatory cytokines, likely via NF-κB (65–67) — exacerbates pathogenesis in a mouse model of HD (68). Consistent with these findings, we recently found that CB2 signaling in immune cells mediates the onset and severity of symptoms in BACHD mice and that CB2 agonists are neuroprotective in R6/2 mice, even when given at late disease stages (69). Finally, inhibition of kynurenine 3-monooxygenase (KMO) in blood cells prevented synaptic loss and brain inflammation and increased lifespan in R6/2 mice (56). Together these findings support a critical link between blood cells and neurodegeneration in HD.

In summary, our study provides in vitro and in vivo evidence for motility and migration deficits in immune cells from HD patients and mouse models. These deficits may partially explain the early immune dysfunction and chronic elevation of proinflammatory cytokines and chemokines in this disease. Immune cell migration

impairment is known to cause recurrent infections and immune dysregulation (34, 70). Further studies to monitor the innate and adaptive immune responses in HD mouse models and patients are warranted. Therapeutic approaches currently used to lower proinflammatory cytokines, including antibodies to TNF-α and IL-6, might provide some benefits to HD patients and should be investigated in mouse models of HD. More broadly, disease-causing proteins in many neurodegenerative diseases caused by polyQ expansions are expressed ubiquitously, and the functional consequences of this expression in non-neuronal cells, including immune cells, merits further investigation.

Methods

Mice and breeding strategy

YAC128 founder mice (35) (FVB/NJ background) were provided by Blair Leavitt (University of British Columbia, Vancouver, Canada). BACHD founder mice (36) (C57BL/6 or FVB/NJ background) were provided by William Yang (UCSD, San Diego, California, USA). *CD11b-Cre* mice (C57BL/6 background) (44) were provided by Don Cleveland (UCSD, San Diego, California, USA) and George Kollias (Biomedical Sciences Research Centre "Alexander Fleming," Vari, Greece). These mice were crossed with WT breeder mice to generate litters as required and crossed with BACHD mice (C57BL/6 background) to generate BACHD;*CD11b-Cre* mice. *Cx3cr1*$^{GFP/GFP}$ mice (C57BL/6 background) (71) were provided by Israel Charo (Gladstone Institute of Cardiovascular Disease, San Francisco, California, USA) and crossed with BACHD mice (C57BL/6 background) to generate BACHD$^{Tg/+}$*Cx3cr1*$^{GFP/+}$ mice for in vivo imaging using 2-photon microscopy.

Cell culture

Primary microglia were isolated from mice on P1–P3 as described previously (71). Briefly, cortices were isolated, trypsinized, triturated into single cells, and cultured in Dulbecco's modified Eagle's medium with high glucose (DME-H21), 10% heat-inactivated FBS, GM-CSF (2 ng/ml), and penicillin/streptomycin. After 10–20 days, cultures were gently shaken by hand, and floating cells (microglia) were collected, resulting in more than 99% purity. GM-CSF (2 ng/ml) was used to help stimulate microglial yield. Isolated cells were incubated with serum-free macrophage medium (Invitrogen) for 24 hours, unless otherwise specified, and used for various experiments. Microglial cell lines BV2 and N9 were stably transduced with lentiviral constructs expressing exon 1 htt 25Q or 72Q, fused to GFP, based on pRRL-cPPT-CMV-X-PRE-SIN (72). Gene insertions and protein expression levels of htt exon 1 were quantified to ensure matched expression levels in microglial cell lines that express htt 25Q and 72Q (data not shown). Cells were cultured in DME-H21 with 5% heat-inactivated FBS.

Chemotaxis assays of microglial cells

Boyden chamber assays. Microglial cell lines and isolated primary microglia were collected and prepared as described previously (40). Briefly, harvested cells were stained with DRAQ5 for 20 minutes and washed with MEM, then with MEM with 10% Cellgro (Mediatech). Migration was measured in a chemotaxis chamber (Neuro Probe) with 10-μm pore filters. Lower wells were filled with chemoattractants (100 μM ATP, Sigma-Aldrich; 100 nM complement protein C5a, Calbiochem). Primary microglia were allowed to migrate from upper wells through the filter for 3 hours at 37°C and 5% CO_2. Nonmigrated cells on top of the filter were wiped off, and the filter was scanned and analyzed with an Odyssey Infrared Imaging System (LI-COR).

Dunn chamber assay. Cells were spotted onto fibronectin-coated coverslips (BD) and incubated with serum-free DME-H21 for 4 hours as described previously (38). The Dunn chamber was used to form an ATP gradient of 0–100 μM. Distance and direction of movement by the cell's leading edge were monitored for 30 minutes by time-lapse microscopy. Images were processed and analyzed with ImageJ software (manual tracking and chemotaxis plug-ins).

In vivo imaging of microglia

EGFP-expressing microglia were imaged in vivo using 2-photon laser scanning fluorescence microscopy as described previously (30). Briefly, mice were anesthetized intraperitoneally with ketamine (200 mg/kg body weight) and xylazine (30 mg/kg body weight) in 0.9% NaCl solution. Transcranial imaging was performed through a thinned region of the skull (~1 mm in diameter) over barrel or motor cortex. A drop (~200 μl) of artificial mouse cerebrospinal fluid (ACSF) was applied on the exposed region for the duration of the experiment. Imaging was performed using an Ultima-IV in vivo microscope (Prairie Technologies) equipped with a MaiTai DeepSee-eHP laser (Spectra Physics). The excitation wavelength was tuned to 915 nm, and imaging was performed from the surface to approximately 200 μm below the pia using an Olympus ×40 0.8-NA water immersion lens. For time-lapse imaging, a *z*-stack of images was acquired every 30–180 seconds, typically over 10–60 minutes. A highly localized injury was achieved by focusing a 2-photon laser beam (~1 μm in size) at a specific point in the cortex through the thinned skull. A maximum intensity projection of each *z*-stack was constructed for each time point and used for quantification of microglial basal process dynamics or their responses following laser ablation. Results were analyzed by determining the change in GFP fluorescence as the processes entered the space surrounding the center of the laser ablation. The fluorescence was normalized to an outer region (3 times the area of the space around the ablation).

Thioglycollate-induced peritonitis

Peritonitis was induced with thioglycollate (Sigma-Aldrich) as described previously (73). Mice were treated with an intraperitoneal injection of 3% thioglycollate or saline control. Peritoneal leukocytes were collected 24 hours later (48 hours for aged mice) by flushing the peritoneal cavity with 10 ml PBS. Peritoneal cells were washed with staining buffer (PBS with 5% FBS), blocked with anti-CD16/32 (1:200, R&D Systems), and stained with anti-F4/80–APC (1:100, Caltag), anti-CD11b–PE (1:500, BD Biosciences — Pharmingen), and anti–Gr-1 (1:100, eBioscience). Cells were analyzed by LSR II (BD Biosciences) and FlowJo software (Tree Star). To quantify the percentage of infiltrating macrophages, we gated cells for the F4/80^{dim} population among unstained and F4/80^{dim} cells. Cells were gated for the Gr-1^{hi} population among CD11b-positive cells in order to quantify the percentage of infiltrating neutrophils.

Isolation of human blood monocytes and macrophages

Blood samples were obtained from control subjects and patients with genetically diagnosed HD and processed as described previously (10). The patients were clinically assessed by a neurologist experienced in assessment of HD patients. The number, age, CAG repeat, and age of onset for each experimental group are described in Supplemental Tables 1 and 2. Monocyte samples for MCP-1 stimulation were from a patient group different from those providing samples for ATP and C5a stimulations. There was also only a partial overlap of patient samples in macrophage experiments for MCP-1 and ATP/C5a treatments. Presymptomatic patients are classified as patients with a positive predictive HD gene test, presenting without clinical feature. Patients were staged under the Shouldon and Fahn scale: early-stage HD patients (disease stages I and II) had united Huntington's disease rating scale (UHDRS) total functional capacity score less than 7, and moderate-stage HD patients (stage III and IV) had total functional capacity score 1–6.

Mononuclear cells were isolated from blood samples using Histopaque-1077 tubes (Sigma-Aldrich), stained with anti-CD14 beads, incu-

bated for 15 minutes at 4°C, washed, resuspended in 500 μl MACS buffer (0.5% FCS and 2 mM EDTA in PBS), and sorted using MACS columns. Isolated monocytes were counted and used for experiments and were 85%–95% $CD14^+$ cells. Macrophages were derived by seeding monocytes onto 24-well plates in 1 ml of culture medium (RPMI with 10% FCS, 2 mM L-glutamine, 50 U/ml penicillin, and 50 μg/ml streptomycin) supplemented with 20 ng/ml recombinant human GM-CSF to induce macrophage differentiation. The medium was changed 3 days after seeding, and cells developed the macrophage phenotype after 6 days in culture.

Chemotaxis assays of human HD monocyte and macrophages

The lower chamber of the Transwell was filled with ATP (100 μM), C5a (10 nM), or MCP-1 (50 ng/ml). Monocytes were placed on 5-μm Transwell inserts and incubated for 1.5 hours at 37°C. Cells that migrated were collected from the lower chamber and counted with a Neubauer counting chamber. Macrophages were seeded onto 0.8-μm Transwell inserts, stimulated with chemoattractants as above, and incubated for 16 hours. Cells on the upper side of the insert membrane were gently removed with cotton swabs; cells on the lower side were fixed in ethanol and stained with 1 mg/ml crystal violet. Migrated cells were counted by light microscopy.

Membrane ruffling

Assays were performed as described previously (38) by culturing the cells on poly-L-lysine (10 μg/ml) and incubating them in macrophage serum-free medium containing ATP (100 μM) or M-CSF (100 ng/ml) for 10 minutes at 37°C. Cells were fixed with 4% paraformaldehyde and stained with rhodamine-conjugated phalloidin (Molecular Probes, Invitrogen). Cells with membrane ruffling, in which cell edges are densely stained, were counted as the percentage of the cells in the field of view.

Western blot analysis

Cells were lysed with standard RIPA buffer (150 mM NaCl, 1% NP-40, 0.1% sodium dodecyl sulfate, 0.5% sodium deoxycholate, 50 mM Tris, pH 7.4) supplemented with complete protease inhibitors (Roche). Proteins were separated by SDS-PAGE, transferred onto a nitrocellulose membrane (Schleicher & Schuell), and blocked for 1 hour with 0.1% Tween and 5% nonfat dry milk. The membrane was probed overnight with the following primary antibodies: anti–p-cofilin (1:1,000, Cell Signaling Technology), anti-cofilin (1:1,000, Cell Signaling Technology/Abcam), and anti-GAPDH (1:500, Chemicon). Cells were then washed and incubated for 1 hour with horseradish peroxidase–conjugated anti-rabbit or anti-mouse (1:10,000). After washing, proteins were detected with ECL kits as directed by the manufacturer (Amersham).

Quantitative PCR

Total RNA was isolated from microglial cells and mouse peritoneal macrophages with the RNeasy Mini Kit (Qiagen). mRNA was reverse-transcribed with Multiscribe Reverse Transcriptase (RT) (Applied Biosystems) according to the manufacturer's instructions. Quantitative RT-PCR was performed in triplicate with Roche Universal Probe Library primers as recommended by the manufacturer (https://www.roche-applied-science.com/sis/rtpcr/upl/index.jsp) and SYBR Green/Fast SYBR Green mix (Applied Biosystems) with a PRISM 7500 quantitative PCR system (Applied Biosystems). Mutant htt primer sequences were: forward 5′-CCGCTCAGGTTCTGCTTTTA-3′, reverse 5′-GCCTTCATCAGCTTTTCCAG-3′. Purity of mRNA was checked by performing quantitative PCR without prior RT. Results were normalized against the housekeeping gene *ATP5* (74).

Statistics

Statistical analyses were performed with GraphPad Prism Software. For pairwise comparison, 1-tailed unpaired Student's *t* test was used, since we tested our hypotheses in one direction (i.e., decrease in migration). For group analysis, ANOVA with Bonferroni's post hoc test was used. Data are presented as mean ± SEM. *P* values less than 0.05 were considered significant.

Study approval

Mice were maintained and bred in accordance with NIH guidelines. All experiments with mice were approved by the Institutional Animal Care and Use Committee of the University of California, San Francisco. Experiments with human samples were conducted in accordance with the Declaration of Helsinki and approved by the UCL/UCL Hospitals Joint Research Ethics Committee, London, United Kingdom. All subjects provided informed written consent. All subjects in the study underwent subject inclusion criteria and were evaluated by HD clinical assessments.

Acknowledgments

We thank Diane Barber for the cofilin and p-cofilin antibodies for initial pilot studies and the UCSF Nikon Imaging Center for assistance with in vitro microscopy. We also thank G. Howard and S. Ordway for editorial assistance. This study was supported by the J. David Gladstone Institutes; NIH grants AG022074 and NS057715 (to P.J. Muchowski), NS051470, NS052189, and NS066361 (to K. Akassoglou); the CHDI Foundation (to P.J. Muchowski and T. Möller); the Taube-Koret Center for Huntington's Disease Research (to P.J. Muchowski); a National Multiple Sclerosis Society fellowship (to D. Davalos); and a Postgraduate Scholarship from the Natural Sciences and Engineering Research Council, Canada (to W. Kwan).

Received for publication April 25, 2012, and accepted in revised form September 27, 2012.

Address correspondence to: Paul J. Muchowski, Gladstone Institute of Neurological Disease, 1650 Owens Street, San Francisco, California 94158, USA. Phone: 415.734.2515; Fax: 415.355.0824; E-mail: pmuchowski@gladstone.ucsf.edu.

Aaron Miller's present address is: Department of Natural Sciences, Concordia University Wisconsin, Mequon, Wisconsin, USA.

Flaviano Giorgini's present address is: Department of Genetics, University of Leicester, Leiceister, United Kingdom.

1. Sassone J, Colciago C, Cislaghi G, Silani V, Ciammola A. Huntington's disease: the current state of research with peripheral tissues. *Exp Neurol*. 2009; 219(2):385–397.
2. van der Burg JM, Bjorkqvist M, Brundin P. Beyond the brain: widespread pathology in Huntington's disease. *Lancet Neurol*. 2009;8(8):765–774.
3. Hult S, et al. Mutant huntingtin causes metabolic imbalance by disruption of hypothalamic neurocircuits. *Cell Metab*. 2011;13(4):428–439.
4. Bjorkqvist M, et al. The R6/2 transgenic mouse model of Huntington's disease develops diabetes due to deficient beta-cell mass and exocytosis. *Hum Mol Genet*. 2005;14(5):565–574.
5. Propert DN. Presymptomatic detection of Huntington's disease. *Med J Aust*. 1980;1(12):609–612.
6. Lodi R, et al. Abnormal in vivo skeletal muscle energy metabolism in Huntington's disease and dentatorubropallidoluysian atrophy. *Ann Neurol*. 2000;48(1):72–76.
7. Aziz NA, van der Burg JM, Landwehrmeyer GB, Brundin P, Stijnen T, Roos RA. Weight loss in Huntington disease increases with higher CAG repeat number. *Neurology*. 2008;71(19):1506–1513.
8. Moscovitch-Lopatin M, et al. Optimization of an HTRF assay for the detection of soluble mutant Huntingtin in human buffy coats: a potential biomarker in blood for Huntington disease. *PLoS Curr*. 2010;2:RRN1205.
9. Leblhuber F, et al. Activated immune system in patients with Huntington's disease. *Clin Chem Lab Med*. 1998;36(10):747–750.
10. Dalrymple A, et al. Proteomic profiling of plasma in Huntington's disease reveals neuroinflammatory activation and biomarker candidates. *J Proteome Res*. 2007;6(7):2833–2840.

11. Bjorkqvist M, et al. A novel pathogenic pathway of immune activation detectable before clinical onset in Huntington's disease. *J Exp Med*. 2008; 205(8):1869–1877.
12. Wild E, et al. Abnormal peripheral chemokine profile in Huntington's disease. *PLoS Curr*. 2011; 3:RRN1231.
13. Anderson AN, Roncaroli F, Hodges A, Deprez M, Turkheimer FE. Chromosomal profiles of gene expression in Huntington's disease. *Brain*. 2008; 131(pt 2):381–388.
14. Borovecki F, et al. Genome-wide expression profiling of human blood reveals biomarkers for Huntington's disease. *Proc Natl Acad Sci U S A*. 2005; 102(31):11023–11028.
15. Runne H, et al. Analysis of potential transcriptomic biomarkers for Huntington's disease in peripheral blood. *Proc Natl Acad Sci U S A*. 2007; 104(36):14424–14429.
16. Kwan W, et al. Bone marrow transplantation confers modest benefits in mouse models of Huntington's disease. *J Neurosci*. 2012;32(1):133–142.
17. Sapp E, et al. Early and progressive accumulation of reactive microglia in the Huntington disease brain. *J Neuropathol Exp Neurol*. 2001;60(2):161–172.
18. Vonsattel JP, Myers RH, Stevens TJ, Ferrante RJ, Bird ED, Richardson EP. Neuropathological classification of Huntington's disease. *J Neuropathol Exp Neurol*. 1985;44(6):559–577.
19. Simmons DA, Casale M, Alcon B, Pham N, Narayan N, Lynch G. Ferritin accumulation in dystrophic microglia is an early event in the development of Huntington's disease. *Glia*. 2007;55(10):1074–1084.
20. Lotharius J, et al. Progressive degeneration of human mesencephalic neuron-derived cells triggered by dopamine-dependent oxidative stress is dependent on the mixed-lineage kinase pathway. *J Neurosci*. 2005;25(27):6329–6342.
21. Tai YF, et al. Microglial activation in presymptomatic Huntington's disease gene carriers. *Brain*. 2007;130(pt 7):1759–1766.
22. Tai YF, et al. Imaging microglial activation in Huntington's disease. *Brain Res Bull*. 2007;72(2–3):148–151.
23. Politis M, et al. Microglial activation in regions related to cognitive function predicts disease onset in Huntington's disease: a multimodal imaging study. *Hum Brain Mapp*. 2011;32(2):258–270.
24. Luster AD, Alon R, von Andrian UH. Immune cell migration in inflammation: present and future therapeutic targets. *Nat Immunol*. 2005;6(12):1182–1190.
25. Madri JA, Graesser D. Cell migration in the immune system: the evolving inter-related roles of adhesion molecules and proteinases. *Dev Immunol*. 2000;7(2–4):103–116.
26. Stossel TP. On the crawling of animal cells. *Science*. 1993;260(5111):1086–1094.
27. Jones GE. Cellular signaling in macrophage migration and chemotaxis. *J Leukoc Biol*. 2000;68(5):593–602.
28. Inoue K. Microglial activation by purines and pyrimidines. *Glia*. 2002;40(2):156–163.
29. Koizumi S, et al. UDP acting at P2Y6 receptors is a mediator of microglial phagocytosis. *Nature*. 2007; 446(7139):1091–1095.
30. Davalos D, et al. ATP mediates rapid microglial response to local brain injury in vivo. *Nat Neurosci*. 2005;8(6):752–758.
31. Nimmerjahn A, Kirchhoff F, Helmchen F. Resting microglial cells are highly dynamic surveillants of brain parenchyma in vivo. *Science*. 2005; 308(5726):1314–1318.
32. Wake H, Moorhouse AJ, Jinno S, Kohsaka S, Nabekura J. Resting microglia directly monitor the functional state of synapses in vivo and determine the fate of ischemic terminals. *J Neurosci*. 2009; 29(13):3974–3980.
33. Kurihara T, Warr G, Loy J, Bravo R. Defects in macrophage recruitment and host defense in mice lacking the CCR2 chemokine receptor. *J Exp Med*. 1997;186(10):1757–1762.
34. Blundell MP, Worth A, Bouma G, Thrasher AJ. The Wiskott-Aldrich syndrome: the actin cytoskeleton and immune cell function. *Dis Markers*. 2010; 29(3–4):157–175.
35. Slow EJ, et al. Selective striatal neuronal loss in a YAC128 mouse model of Huntington disease. *Hum Mol Genet*. 2003;12(13):1555–1567.
36. Gray M, et al. Full-length human mutant huntingtin with a stable polyglutamine repeat can elicit progressive and selective neuropathogenesis in BACHD mice. *J Neurosci*. 2008;28(24):6182–6195.
37. Blasi E, Barluzzi R, Bocchini V, Mazzolla R, Bistoni F. Immortalization of murine microglial cells by a v-raf/v-myc carrying retrovirus. *J Neuroimmunol*. 1990;27(2–3):229–237.
38. Haynes SE, et al. The P2Y12 receptor regulates microglial activation by extracellular nucleotides. *Nat Neurosci*. 2006;9(12):1512–1519.
39. Irino Y, Nakamura Y, Inoue K, Kohsaka S, Ohsawa K. Akt activation is involved in P2Y12 receptor-mediated chemotaxis of microglia. *J Neurosci Res*. 2008;86(7):1511–1519.
40. Miller AM, Stella N. Microglial cell migration stimulated by ATP and C5a involve distinct molecular mechanisms: quantification of migration by a novel near-infrared method. *Glia*. 2009;57(8):875–883.
41. McKercher SR, et al. Targeted disruption of the PU.1 gene results in multiple hematopoietic abnormalities. *EMBO J*. 1996;15(20):5647–5658.
42. Ransohoff RM, Cardona AE. The myeloid cells of the central nervous system parenchyma. *Nature*. 2010;468(7321):253–262.
43. Ginhoux F, et al. Fate mapping analysis reveals that adult microglia derive from primitive macrophages. *Science*. 2010;330(6005):841–845.
44. Boillee S, et al. Onset and progression in inherited ALS determined by motor neurons and microglia. *Science*. 2006;312(5778):1389–1392.
45. Ohsawa K, Imai Y, Kanazawa H, Sasaki Y, Kohsaka S. Involvement of Iba1 in membrane ruffling and phagocytosis of macrophages/microglia. *J Cell Sci*. 2000;113(pt 17):3073–3084.
46. Imai Y, Kohsaka S. Intracellular signaling in M-CSF-induced microglia activation: role of Iba1. *Glia*. 2002;40(2):164–174.
47. Dawe HR, Minamide LS, Bamburg JR, Cramer LP. ADF/cofilin controls cell polarity during fibroblast migration. *Curr Biol*. 2003;13(3):252–257.
48. Wang Y, Shibasaki F, Mizuno K. Calcium signal-induced cofilin dephosphorylation is mediated by Slingshot via calcineurin. *J Biol Chem*. 2005; 280(13):12683–12689.
49. Munsie L, et al. Mutant Huntingtin causes defective actin remodeling during stress: defining a new role for transglutaminase 2 in neurodegenerative disease. *Hum Mol Genet*. 2011;20(10):1937–1951.
50. Ma L, Morton AJ, Nicholson LF. Microglia density decreases with age in a mouse model of Huntington's disease. *Glia*. 2003;43(3):274–280.
51. Lynch G, et al. Brain-derived neurotrophic factor restores synaptic plasticity in a knock-in mouse model of Huntington's disease. *J Neurosci*. 2007; 27(16):4424–4434.
52. Reis SA, et al. Striatal neurons expressing full-length mutant huntingtin exhibit decreased N-cadherin and altered neuritogenesis. *Hum Mol Genet*. 2011;20(12):2344–2355.
53. Myre MA, Lumsden AL, Thompson MN, Wasco W, Macdonald ME, Gusella JF. Deficiency of huntingtin has pleiotropic effects in the social amoeba Dictyostelium discoideum. *PLoS Genet*. 2011; 7(4):e1002052.
54. Pascual O, Ben Achour S, Rostaing P, Triller A, Bessis A. Microglia activation triggers astrocyte-mediated modulation of excitatory neurotransmission. *Proc Natl Acad Sci U S A*. 2011;109(4):E197–E205.
55. Cardona AE, et al. Control of microglial neurotoxicity by the fractalkine receptor. *Nat Neurosci*. 2006;9(7):917–924.
56. Zwilling D, et al. Kynurenine 3-monooxygenase inhibition in blood ameliorates neurodegeneration. *Cell*. 2011;145(6):863–874.
57. Goodman JC, Van M, Gopinath SP, Robertson CS. Pro-inflammatory and pro-apoptotic elements of the neuroinflammatory response are activated in traumatic brain injury. *Acta Neurochir Suppl*. 2008; 102:437–439.
58. Chaparro-Huerta V, Rivera-Cervantes MC, Flores-Soto ME, Gomez-Pinedo U, Beas-Zarate C. Pro-inflammatory cytokines and apoptosis following glutamate-induced excitotoxicity mediated by p38 MAPK in the hippocampus of neonatal rats. *J Neuroimmunol*. 2005;165(1–2):53–62.
59. Rogers JT, et al. CX3CR1 deficiency leads to impairment of hippocampal cognitive function and synaptic plasticity. *J Neurosci*. 2011;31(45):16241–16250.
60. Rampersad RR, et al. Enhanced Th17-cell responses render CCR2-deficient mice more susceptible for autoimmune arthritis. *PLoS One*. 2011;6(10):e25833.
61. Ishida Y, Gao JL, Murphy PM. Chemokine receptor CX3CR1 mediates skin wound healing by promoting macrophage and fibroblast accumulation and function. *J Immunol*. 2008;180(1):569–579.
62. Boring L, et al. Impaired monocyte migration and reduced type 1 (Th1) cytokine responses in C-C chemokine receptor 2 knockout mice. *J Clin Invest*. 1997; 100(10):2552–2561.
63. Christensen PJ, et al. Expression and functional implications of CCR2 expression on murine alveolar epithelial cells. *Am J Physiol Lung Cell Mol Physiol*. 2004;286(1):L68–L72.
64. Lanska DJ, Lanska MJ, Lavine L, Schoenberg BS. Conditions associated with Huntington's disease at death. A case-control study. *Arch Neurol*. 1988; 45(8):878–880.
65. Herring AC, Koh WS, Kaminski NE. Inhibition of the cyclic AMP signaling cascade and nuclear factor binding to CRE and kappaB elements by cannabinol, a minimally CNS-active cannabinoid. *Biochem Pharmacol*. 1998;55(7):1013–1023.
66. Ehrhart J, et al. Stimulation of cannabinoid receptor 2 (CB2) suppresses microglial activation. *J Neuroinflammation*. 2005;2:29.
67. Mukhopadhyay S, et al. Lipopolysaccharide and cyclic AMP regulation of CB(2) cannabinoid receptor levels in rat brain and mouse RAW 264.7 macrophages. *J Neuroimmunol*. 2006;181(1–2):82–92.
68. Palazuelos J, et al. Microglial CB2 cannabinoid receptors are neuroprotective in Huntington's disease excitotoxicity. *Brain*. 2009;132(pt 11):3152–3164.
69. Bouchar J, et al. Cannabinoid receptor 2 signaling in peripheral immune cells modulates disease onset and severity in mouse models of Huntington's disease. *J Neurosci*. In press.
70. Etzioni A, et al. Brief report: recurrent severe infections caused by a novel leukocyte adhesion deficiency. *N Engl J Med*. 1992;327(25):1789–1792.
71. Jung S, et al. Analysis of fractalkine receptor CX(3) CR1 function by targeted deletion and green fluorescent protein reporter gene insertion. *Mol Cell Biol*. 2000;20(11):4106–4114.
72. Balcaitis S, Weinstein JR, Li S, Chamberlain JS, Moller T. Lentiviral transduction of microglial cells. *Glia*. 2005;50(1):48–55.
73. Saederup N, et al. Selective chemokine receptor usage by central nervous system myeloid cells in CCR2-red fluorescent protein knock-in mice. *PLoS One*. 2010;5(10):e13693.
74. Benn CL, Fox H, Bates GP. Optimisation of region-specific reference gene selection and relative gene expression analysis methods for pre-clinical trials of Huntington's disease. *Mol Neurodegener*. 2008;3:17.